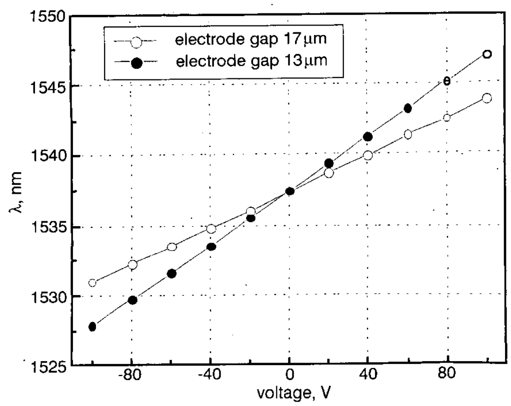

Fig. 3 *Tuning of centre wavelength of drop channel (port 4) with applied voltage*

Acknowledgments: This work was sponsored by the Texas Advanced Technology Program, Lockheed Martin, and 3M.

20 November 2001
Electronics Letters Online No: 20020162
DOI: 10.1049/el:20020162

Pingsheng Tang, O. Eknoyan and H.F. Taylor (*Department of Electrical Engineering, Texas A&M University, College Station, TX 77843-3128, USA*)

References

1 KEISER, G.E.: 'A review of WDM technology and applications' *in* Optical fiber technology' (Academic Press, New York, 1999, Vol. 5), pp. 3–39
2 ELMIRGHANI, J.M.H., and MOUFTAH, H.T.: 'Technologies and architecture for scalable dynamic dense WDM networks', *IEEE Commun. Mag.*, 2000, **38**, pp. 58–66
3 SADOT, D., and BOIMOVICH, E.: 'Tunable optical filters for dense WDM networks', *IEEE Commun. Mag.*, 1998, **36**, pp. 50–55
4 GREEN, JR., P.E.: 'Fiber optic networks' (Prentice Hall, Englewood Cliffs, NJ, 1993), Chap. 4
5 WARZANSKI, W., HEISMANN, F., and ALFERNESS, R.C.: 'Polarization-independent electro-optically tunable narrow-band wavelength filter', *Appl. Phys. Lett.*, 1988, **30**, pp. 13–15
6 TANG, Z., EKNOYAN, O., and TAYLOR, H.F.: 'Polarisation-independent electro-optically tunable wavelength filter in $LiTaO_3$', *Electron. Lett.*, 1994, **30**, pp. 1758–1759
7 WEHERMANN, F., HARIZI, C., HERRMANN, H., RUST, U., SOHLER, W., and WESTENHÖFER, S.: 'Integrated optical, wavelength selective, acoustically tunable 2 × 2 switches (add-drop multiplexers) in $LiNbO_3$', *IEEE J. Sel. Top. Quantum Electron.*, 1996, **2**, pp. 263–269
8 CROSTON, I.R., CARR, A.D., PARSONS, N.J., RADCLIFFE, S.N., and ST. VILLE, L.S.: 'Lithium niobate electro-optic tunable filter with high sidelobe suppression', *Electron. Lett.*, 1993, **29**, pp. 157–159

Automatic repeat request schemes for infrared wireless communications

V. Vitsas and A.C. Boucouvalas

The effectiveness of employing a stop-and-wait automatic repeat request protocol as well as a go-back-*N* protocol to cope with transmission errors in infrared wireless connections is examined. Protocol performance for various link parameters, such as window size, packet size and timer time-out values is presented. High window size implementation results in better performance.

Introduction: The increasing number of laptop computers on the market creates a demand for their wireless connectivity. The Infrared Data Association (IrDA) has been very successful in developing standards for wireless indoor point-to-point connections using the unregulated infrared spectrum [1]. It is a remarkable achievement for the IrDA 1.x standard to establish such a widespread deployment in such a wide range of devices within a relatively short time [2]. IrDA recently proposed the advanced infrared (AIr) standard for indoor optical wireless LANs. The AIr standard employs the IrDA 1.x protocol stack. A new physical layer (AIr-PHY) is proposed that employs wide angle infrared ports [2]. IrLAP, the IrDA 1.x data link layer, was split into three sub-layers, the AIr medium access control (AIr-MAC), the AIr link manager (AIr-LM) and the AIr link control (AIr-LC) sub-layers [3]. IrDA 1.x IrLAP performance is examined in [4, 5]. In this Letter we report our examination of an AIr IrLAP performance evaluation. AIr-MAC is a carrier sense multiple access with collision avoidance (CSMA/CA) protocol employing a request-to-send/clear-to-send (RTS/CTS) reservation scheme to address the hidden station problem [2]. A successful reservation is always terminated by means of an end-of-burst/end-of-burst confirm (EOB/EOBC) packet exchange. Infrared link quality is affected detrimentally by background ambient light, sunlight and diffuse propagation paths, and physical obstacles cause loss of line of sight. To improve link quality, the AIr-LC sub-layer utilises a go-back-*N* (GBN) automatic repeat request (ARQ) retransmission scheme and the AIr-MAC sub-layer utilises an optional stop-and-wait (SW) ARQ scheme [3]. We also investigated the effectiveness of employing the SW ARQ scheme at the MAC layer when the GBN ARQ scheme at the LC layer is implemented. The packet level acknowledgment (PLACK) protocol utilises the GBN ARQ scheme at the LC layer and the SW ARQ scheme at the MAC layer. The no packet level acknowledgment (NoPLACK) protocol utilises the GBN ARQ scheme at the LC layer and the no ARQ scheme at the MAC layer. Analytical models for the utilisation of the PLACK and NoPLACK protocols are presented. PLACK is compared to NoPLACK performance for different parameter values.

Analysis: The utilisation of the PLACK protocol, U_{PLACK}, is calculated first. For packet error rate (PER) p_e and window size w, the probability $P_{s/i}$ that i reservations are needed to successfully transmit all packets is given by

$$P_{s/i} = \frac{(w+i-2)!}{(i-1)!(w-1)!}(1-p_e)^w p_e^{i-1} \quad (1)$$

We have calculated the total time required, I_D, for a complete window transmission

$$I_D = \sum_{i=1}^{\infty} P_{s/i}(i(C_p + D) + (w+i-1)(t+F+2d+p_1+E)) \quad (2)$$

where C_p is the average contention period, D is the total transmission time of the RTS/CTS/EOB/EOBC packets, t is the payload data transmission time, F is the data packet overhead transmission time, d is the one-way propagation delay, p_1 is the preparation time of a data packet and E is the time required for a packet acknowledgment. The time required for the LC layer acknowledgment (ACK) packet is given by

$$I_A = \sum_{i=1}^{\infty}(1-p_{ack})p_{ack}^{i-1}(i(C_p+D)+i(t_{ack}+2d+p_1+E)) \quad (3)$$

where p_{ack} and t_{ack} are the LC layer ACK packet error rate and transmission time, respectively. U_{PLACK} is given by

$$U_{PLACK} = \frac{wt}{I_D + I_A} \quad (4)$$

The utilisation of the NoPLACK protocol is calculated as follows. The transmission time of data packets and the corresponding acknowledgment, R, is given by.

$$R = 2(C_p + D) + w(t + F + p_1) + p_1 + t_{ack} + p_3 + d \quad (5)$$

where p_3 is the processing time of an acknowledgment and other parameters are the same. The probability, p_i, that either the poll bit or the corresponding final bit are lost i times is given by

$$p_i = (p_e + (1-p_e)p_{ack})(p_{ack} + (1-p_{ack})p_{ack})^{(i-1)} \quad (6)$$

and, I_R, the average window transmission time can be evaluated by

$$I_R = R + \sum_{i=1}^{\infty} p_i(T_t + C_p + D + p_1 + t_{ack} + p_3 + d) \quad (7)$$

where T_t is the LC layer time-out period. NoPLACK protocol utilisation is finally given by [4]:

$$U_{NoPLACK} = t\,\frac{1-p_e}{p_e}\,\frac{(1-(1-p_e)^N)}{l_R} \qquad (8)$$

A utilisation ratio is defined to compare PLACK and NoPLACK protocol performance:

$$U_{ratio} = \frac{U_{NoPLACK}}{U_{PLACK}} \qquad (9)$$

The parameters used are as follows. AIr-MAC specification [3] defines that D, E and F are 1.984 ms, 872 µs and 250 µs, respectively. The processor speed is 100 MHz, p_1 and p_3 values are both 40 ms. The packet length l is 16 Kbytes, the link rate C is 4 Mbit/s, the LC layer ACK transmission time t_{ack} is 250 µs and p_{ack} is approximated by $p_{ack} = p_e(l'/l)$, where $l' = 72$ is the MAC ACK packet length. The one way propagation delay is 0.33 µs and the average contention period C_p is 2.8 ms. The chosen C_p value corresponds to an infrared LAN having only two active stations, the transmitter and the receiver [3].

Results: Fig. 1 compares PLACK and NoPLACK protocol utilisation for different w values. It shows that the AIr protocol practically relies on large window sizes to achieve high channel utilisation. Link utilisation is very low for small window sizes for both protocols caused by the increased number of contention periods and RTS/CTS/EOB/EOBC exchanges. The NoPLACK protocol achieves a higher utilisation for low error rates since it does not spend time transmitting unnecessary (in this case) acknowledgments. The situation is reversed for high error rates as the PLACK protocol immediately realises a packet loss by the absence of the corresponding acknowledgment. Fig. 1 also shows that the employment of larger window size shifts the error rates from which the PLACK protocol outperforms the NoPLACK protocol to higher values.

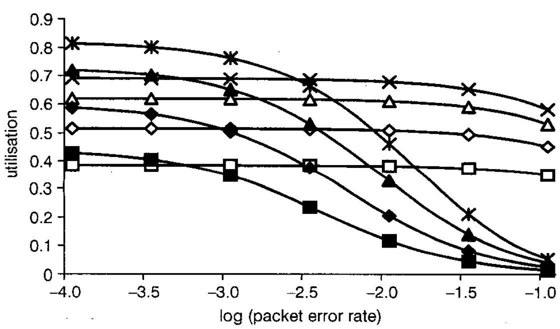

Fig. 1 *Utilisation against packet error rate for various window sizes*
$C_p = 2.8$ ms, $l = 16$ Kbytes, $T_t = 5$ s, $C = 4$ Mbit/s
□ U_{PLACK}, $w = 2$ packets
■ $U_{NoPLACK}$, $w = 2$ packets
◇ U_{PLACK}, $w = 4$ packets
◆ $U_{NoPLACK}$, $w = 4$ packets
△ U_{PLACK}, $w = 8$ packets
▲ $U_{NoPLACK}$, $w = 8$ packets
× U_{PLACK}, $w = 16$ packets
∗ $U_{NoPLACK}$, $w = 16$ packets

Fig. 2 plots U_{ratio} against PER for different LC time-out T_t values. It shows that as T_t decreases, the error rates from which the PLACK protocol outperforms the NoPLACK protocol shift to higher values. PLACK performance is independent of T_t values (4), but NoPLACK performance degrades with an increase in T_t (5) since it relies on the successful transmission of the last data packet to carry the poll to the receiver. If the poll is lost, the situation is resolved by a transmitter's LC T_t expiration.

Fig. 3 shows U_{ratio} against PER for different packet sizes. Increasing packet size when the PER is stable corresponds to better bit error rate. Fig. 3 identifies a specific PER value independent of packet length at which the PLACK and NoPLACK protocol performances are equal. Fig. 3 also shows that decreasing packet length increases the No-PLACK superiority at low PER and also increases the PLACK superiority at high PER.

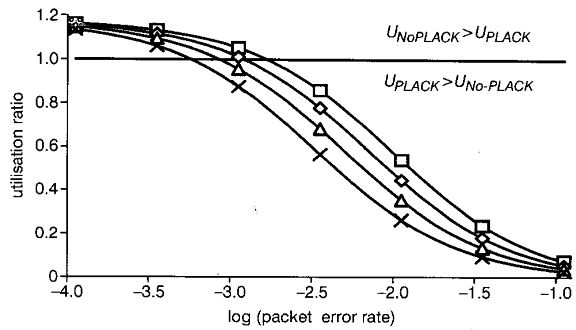

Fig. 2 *Utilisation ratio against packet error rate for various LC time-out values*
$w = 8$ packets, $C_p = 2.8$ ms, $l = 16$ Kbytes, $C = 4$ Mbit/s
□ U_{ratio}, $T_t = 5$ s
◇ U_{ratio}, $T_t = 7$ s
△ U_{ratio}, $T_t = 10$ s
× U_{ratio}, $T_t = 15$ s

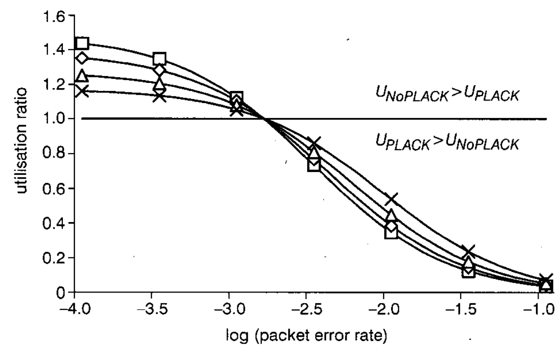

Fig. 3 *Utilisation ratio against packet error rate for various packet sizes l*
$C_p = 2.8$ ms, $w = 8$ packets, $T_t = 5$ s, $C = 4$ Mbit/s
□ U_{ratio}, $l = 2$ Kbits
◇ U_{ratio}, $l = 4$ Kbits
△ U_{ratio}, $l = 8$ Kbits
× U_{ratio}, $l = 16$ Kbits

Conclusions: The AIr protocol should implement large window sizes in order to achieve high channel utilisation. This is due to the large time utilised for contention and for RTS/CTS/EOB/EOBC packet exchange for every successful reservation. The NoPLACK protocol outperforms the PLACK protocol for low error rates. The situation is reversed for high error rates, leading to the conclusion that if some utilisation loss (~10%) is acceptable at low PER, PLACK offers a robust choice. If NoPLACK implementation is chosen, increasing window size and lowering LC time-out values is of great importance.

7 November 2001
Electronics Letters Online No: 20020163
DOI: 10.1049/el:20020163

V. Vitsas and A.C. Boucouvalas (*Multimedia Communications Research Group, School of Design, Engineering and Computing, Bournemouth University, Fern Barrow, Poole, Dorset BH12 5BB, United Kingdom*)

E-mail: tboucouv@bournemouth.ac.uk

References

1 KNUTSON, C., JOOS, D., and WOODINGS, R.: 'Infrared data communications in wireless personal area networks'. Proc. 5th World Multiconf. on Systemics, Cybernetics and Informatics, Orlando, Florida, USA, 2001, Vol. IV, pp. 427–431
2 WILLIAMS, S.: 'IrDA: past, present and future', *IEEE Pers. Commun.*, 2000, 7, (1), pp. 11–19
3 IrDA: 'Advanced infrared (AIr) MAC and AIr LC protocol specifications' (Infrared Data Association, 1999)
4 VITSAS, V., and BOUCOUVALAS, A.C.: 'Simultaneous optimisation of window and frame size for maximum throughput IrDA links', *Electron. Lett.*, 2001, **37**, (16), pp. 1042–1043

5 ROBERTSON, M., HANSEN, S., SORENSON, F., and KNUTSON, C.: 'Modeling IrDA performance: the effect of IrLAP negotiation parameters on throughput'. Proc. 10th IEEE Int. Conf. on Computer Communications and Networks (ICCCN), Phoenix, Arizona, USA, October 2001 pp. 122–127

Peak-to-average power reduction for OFDM by repeated clipping and frequency domain filtering

J. Armstrong

It is shown that repeated clipping and frequency domain filtering of an orthogonal frequency division multiplexing (OFDM) signal can significantly reduce the peak-to-average power ratio (PAPR) of the transmitted signal. The technique causes no increase in out-of-band power. Significant PAPR reduction can be achieved with only moderate levels of clipping noise.

Introduction: One of the main disadvantages of orthogonal frequency division multiplexing (OFDM) is its high peak-to-average power ratio (PAPR). The simplest approach to reducing the PAPR of OFDM signals is to clip the high amplitude peaks. A recent paper [1] described a new clip-and-filter technique that gives better performance than earlier techniques. Like other clip-and-filter techniques, the filtering results in some peak regrowth, so that the final signal will exceed the clipping level at some points. In this Letter it is shown that, with this form of filtering, repeated clip-and-filter operations can be used to reduce the overall peak regrowth.

PAPR reduction by clipping and frequency domain filtering: Fig. 1 shows the block diagram of the basic PAPR reduction scheme [1]. The ith input vector $\mathbf{A}_i = a_{0,i} \cdots a_{N-1,i}$ is first transformed using an oversize inverse fast Fourier transform (IFFT). N is the number of subcarriers in each OFDM symbol. For an oversampling factor of I_1, $\mathbf{A}_i$ is extended by adding $N(I_1 - 1)$ zeros in the middle of the vector. This results in trigonometric interpolation of the time domain signal [1].

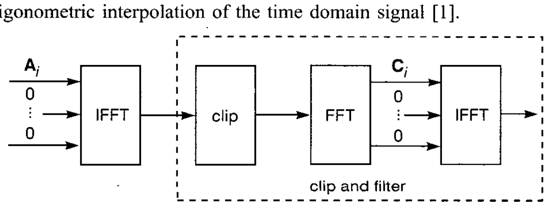

Fig. 1 *Block diagram of peak reduction technique*

The interpolated signal is then clipped. In this Letter, hard-limiting is applied to the amplitude of the complex values at the IFFT output but any other form of nonlinearity could be used. The clipping ratio, *CR*, is defined as the ratio of the clipping level to the root mean square value of the unclipped signal.

The clipping is followed by filtering to reduce out-of-band power. The filter consists of two FFT operations. The forward FFT transforms the clipped signal back into the discrete frequency domain resulting in vector $\mathbf{C}_i$. The in-band discrete frequency components of $\mathbf{C}_i$, $c_{0,i} \cdots c_{N/2-1,i}$, $c_{NI_1-N/2+1,i} \cdots c_{NI_1-1,i}$ are passed unchanged to the inputs of the second IFFT while the out-of-band components, $c_{N/2+1,i} \cdots c_{NI_1-N/2,i}$ are nulled. In systems where some band-edge subcarriers are unused the components corresponding to these are also nulled.

The resulting filter is a time-dependent filter, which passes in-band and rejects out-of-band 'discrete' frequency components. This means that it causes no distortion to the in-band OFDM signal. Since the filter operates on a symbol-by-symbol basis, it causes no intersymbol interference. The filtering does cause some peak regrowth.

Fig. 2 shows the cumulative distribution of the power of the oversampled signal after one to four stages of clipping and filtering. In this case $N = 128$, the modulation is 4-QAM and $CR = 6$ dB. However other parameters would give similar results. Fig. 2 shows that repeated clipping and filtering significantly reduces the PAPR (note the logarithmic scales).

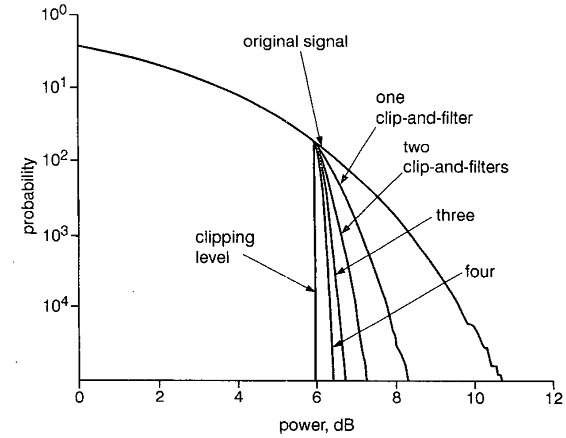

Fig. 2 *Cumulative distribution for signal after PAPR reduction*

In-band distortion: The new clip-and-filter technique causes no increase in out-of-band power so the limit to PAPR reduction in a practical system is the in-band distortion, in the form of clipping noise.

A number of authors have analysed the effects of nonlinearities on OFDM signals [2]. The real and imaginary components of an OFDM signal have Gaussian distributions, thus by extending Bussgang's theory to the complex case it is possible to show that, subject to certain conditions, [2]

$$y(t) = Kx(t) + d(t) \quad (1)$$

where $x(t)$ is the input to the nonlinearity, K is a constant and $y(t)$ is the output. $d(t)$ is a zero mean random noise process which is uncorrelated with $x(t)$, so that

$$E[d^*(t)x(t+\tau)] = 0 \quad (2)$$

$$E[d(t)] = 0 \quad (3)$$

Thus,

$$K = \frac{E[y(t)x^*(t)]}{E[x(t)x^*(t)]} \quad (4)$$

For the case of repeated clipping and filtering Bussgang's theory applies only to the first clipping stage as the input of signals to subsequent clipping stages do not have Gaussian statistics. In the subsequent analysis it is assumed that Bussgang's theory applies, however this may cause second-order errors in the analysis.

In an OFDM system, the output of the nonlinearity, $y(t)$, is the time domain signal at the transmitter output. In the absence of distortion and noise in the channel, samples of sections of $y(t)$ are input to the receiver FFT. Thus the vector output from the FFT for the ith received symbol can be described by

$$\mathbf{Z}_i = K\mathbf{A}_i + \mathbf{B}_i \quad (5)$$

where $\mathbf{B}_i$ is the FFT of the vector of samples of $d(t)$. In this case the signal-to-clipping noise ratio (SCNR) for the kth subcarrier is given by

$$SCNR_k = \frac{K^2 E[(a_{k,i})^2]}{E[(b_{k,i})^2]} \quad (6)$$

where $b_{k,i}$ is the kth element of the noise vector $\mathbf{B}_i$.

In general the SCNR depends on the subcarrier index [2]. In the simulations an average value of the SCNR was calculated. K was estimated by substituting in (6) the measured statistics for the entire simulated sequence. This value of K was then used to calculate the sequence of $\mathbf{B}_i$. Fig. 3 shows the SCNR for various cases. Even for severe clipping, the SCNR is quite large. This is because the main effect of clipping is to reduce K rather than increase the variance of $b_{k,i}$.

The distribution of the real (or imaginary) component of $d(t)$ is in general very non-Gaussian, with a large peak at zero corresponding to input signal values which are below the clipping level, and are therefore not clipped. Despite this, because of the FFT, $b_{k,i}$ may be Gaussian if the central limit theorem applies. This is the case if *CR* is such that there are a significant number of clips per symbol. This will occur at lower *CR* as N increases.